SOLAR POLARIZATION 5
ASP Conference Series, Vol. 405, © 2009
S. V. Berdyugina, K. N. Nagendra, and R. Ramelli, eds.

Fine-scale Stochastic Structure of Solar Magnetic Fields

V. Chertoprud, B. Ioshpa, and V. Obridko

Pushkov Institute of Terrestrial Magnetism, Ionosphere and Radio Wave Propagation, Russian Academy of Sciences, Troitsk, Moscow Region, 142190 Russia

Abstract. Fine-structure ($\sim 10''$) stochastic properties of the magnetic field of the Sun have been analyzed in the frames of a two-dimensional model of the fractal Brownian process (mean square of the field magnitude difference at two points spaced by a distance D is proportional to D^{2H}). The standard deviation s of the magnetic field and the exponent H corresponding to different levels of $\mid B \mid$ have been determined using digitized solar magnetograms with $2''$ resolution (SOHO/MDI, Scherrer et al. 1995). It is established that transition from the background magnetic field to the active region (AR) magnetic fields occurs in the field region 25–50 G. The exponent H has been determined as a function of the magnetic field magnitude. The exponent H for the background magnetic field is essentially smaller than for the AR fields. The relation between the results obtained and some fundamental properties of the behavior of solar plasma (turbulence, convection) are discussed.

1. Data Processing

A two-dimensional model of the fractal Brownian process has been used to describe small-scale ($\sim 10''$) stochastic properties of the solar magnetic field. Within this model, the solar magnetic field $B(x, y)$ at small distances $[(\Delta x^2 + (\Delta y^2)]^{1/2}$ varies as

$$\langle([B(x,y) - B(x+\Delta x, \quad y+\Delta y)]\rangle^2 \infty [\Delta x^2 + \Delta y^2]^H, \tag{1}$$

where the broken brackets $\langle\rangle$ denote the mathematical expectation and $0 < H < 1$ is the Hurst exponent (Potapov 2005) (the smaller is H the rougher is the surface $B(x, y)$).

The procedure of finding the Hurst exponent is reduced to calculating the function $V(L) = \langle([B(x,y) - B(x+\Delta x, \quad y+\Delta y)]\rangle^2$(from magnetographic data (the averaging is performed over all Δx and Δy for which $\Delta x^2 + \Delta y^2 = L$) and estimating the coefficient H in the regression equations

$$\lg V(L) = C + H \lg L \qquad L \leq L_M = d^{1/2} \tag{2}$$

where C is constant and d is the maximum scale used in finding H. Note that, in determining H, we can process the maps with lacunas in the $B(x, y)$ data, which ensures the usefulness of the scheme discussed below.

We have analyzed the central region of the Sun in the range of latitudes $\phi = \pm 30°$ and longitudes $\lambda = \pm 30°$ (from the central meridian) depicted on a 499×499 pixel map (SOHO/MDI, Scherrer et al. 1995). In addition to the original map, we have examined 18 modified versions with $|B|$ confined to one of the 18 levels (A or a) listed below: when the corresponding condition was violated, the $B(x, y)$ value was substituted by a gap.

$$|B| \leq A, \qquad A = 2000, 1500, 1000, 500, 200, 100, 50, 25, 10, 5, 3 \text{ G}; \tag{3}$$

$$|B| \leq a, \qquad a = 25, 50, 100, 150, 200, 250, 300 \text{ G}. \tag{4}$$

The data of the original (non-modified) map obey the condition $|B| \leq A$, $A = 2500\,\text{G}$. For 19 versions of the map under consideration, we determined the standard deviation s of the magnetic field and the Hurst exponent (six estimates with d ranging from $4''$ to $24''$ for each version). All magnetograms for a given day (with the exception of the nonstandard averaged magnetograms marked with an asterisk in the archive SOHO/MDI) were processed following the above scheme, and the daily mean values of s and H were calculated to form the basis for the subsequent analysis.

A 35-day interval (from July 7 to August 10, 2002) with highly variable solar activity and 3 days with low activity (February 13, and May 8 and 14, 2006) have been selected to study the time variation of H. The total of 405 magnetograms for these days were processed. The selected 35-day interval is characterized by large variations in $F_{10.7}$ (from 133 to 249). Large-scale magnetic fields of 3 active regions with a strong field are present on the map. On the three days with low activity, $F_{10.7}$ was equal, respectively, to 74, 86, and 74.

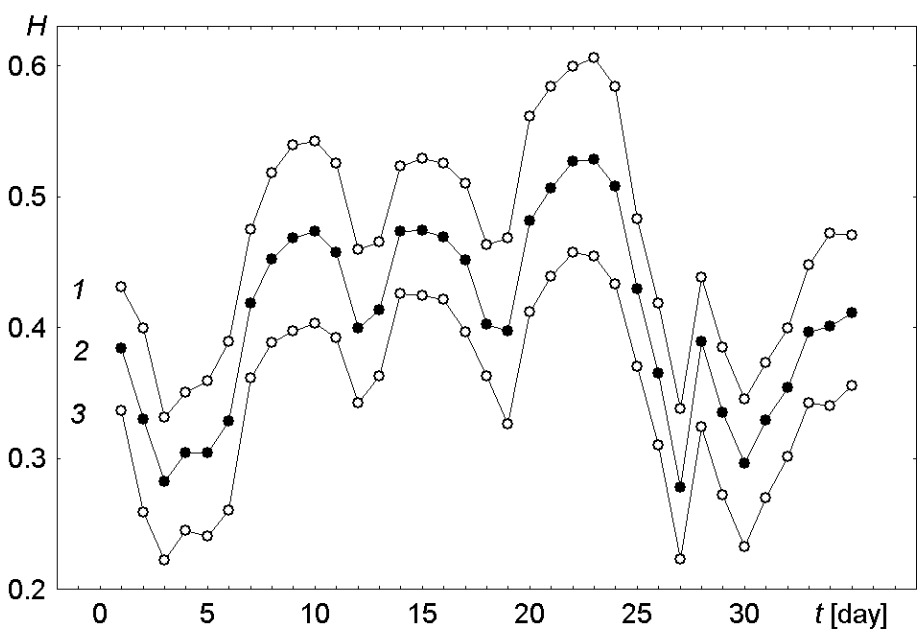

Figure 1. Time variation of the Hurst exponent H. The H values were estimated from the original B data at $d = 4''$ (1), $d = 10''$ (2), and $d = 19''$ (3); $t = 0$ corresponds to July 6, 2002.

As seen from Fig. 1, $B(x, y)$ is not an ideal fractal surface on small scales: as the maximum scale d increases from $4''$ to $24''$, the mean value of H does not remain constant but decreases by one third changing from 0.46 to 0.31. Thus, the roughness of the $B(x, y)$ surface increases with the growth of d, which is, probably, a manifestation of the hierarchy of the magnetic structures.

Let us emphasize some particularities (Fig. 2). Firstly, H virtually stops growing with the increase of $|B|$ as we pass from the level $a = 25\,\mathrm{G}$ to $a = 50\,\mathrm{G}$ and higher. Secondly, the variations of H observed at high levels of $|B|$ and associated with the transition through the central meridian of the active regions can be traced down to low levels and disappear at $A = 25\,\mathrm{G}$.

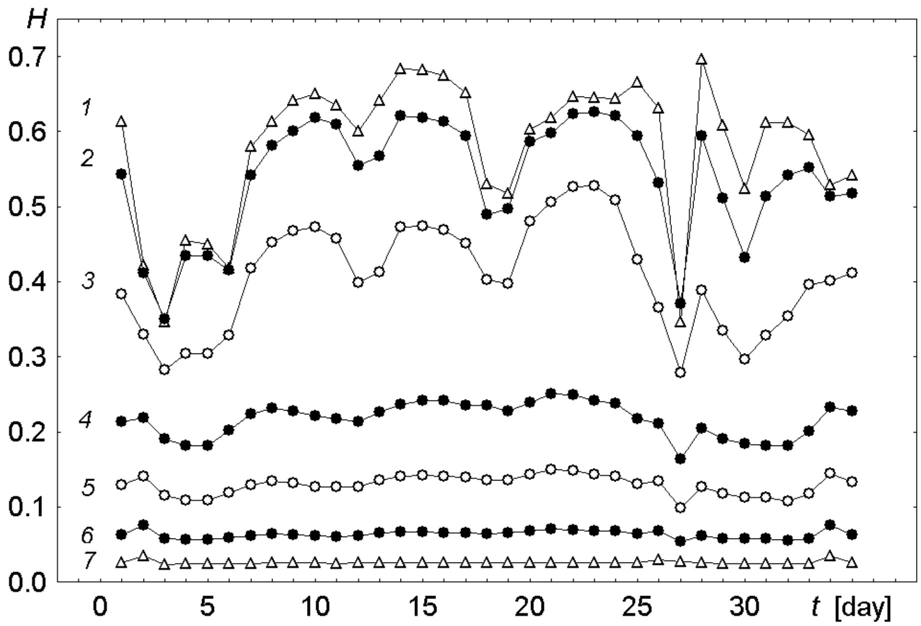

Figure 2. Time variation of the exponent H obtained for different magnetic field levels: 1) $|B| \geq 50\,\mathrm{G}$, 2) $|B| \geq 25\,\mathrm{G}$, 3) $|B| \leq 2500\,\mathrm{G}$, 4) $|B| \leq 200\,\mathrm{G}$, 5) $|B| \leq 100\,\mathrm{G}$, 6) $|B| \leq 50\,\mathrm{G}$, 7) $|B| \leq 25\,\mathrm{G}$; $t = 0$ corresponds to July 6, 2002, and $d = 10''$.

The exponent H is 0.5–0.7 for the active region magnetic fields and $\sim$0.1 for the background field. There are two other notable facts. For the active region magnetic fields, H does not depend significantly on the field amplitude, its estimates being limited to 0.75. Thus, when passing from the background magnetic field to the AR fields, the roughness of the $B(x, y)$ surface decreases but does not disappear completely.

The background $H(s)$ relations for the quiet and disturbed Sun represented in Figs. 3 and 4 agree perfectly well. Thus, the presence of active regions on the Sun seems to have no noticeable effect on the fine-scale structure of the background magnetic field. The data represented in Fig. 3 evidence that the estimates of H and s remain stable when passing from one quiet day to another. A bend in the $H(s)$ curve at $s \approx 10\,\mathrm{G}$ may be the result of reaching the error level, which, in the case under discussion, must be $\sim$6 G.

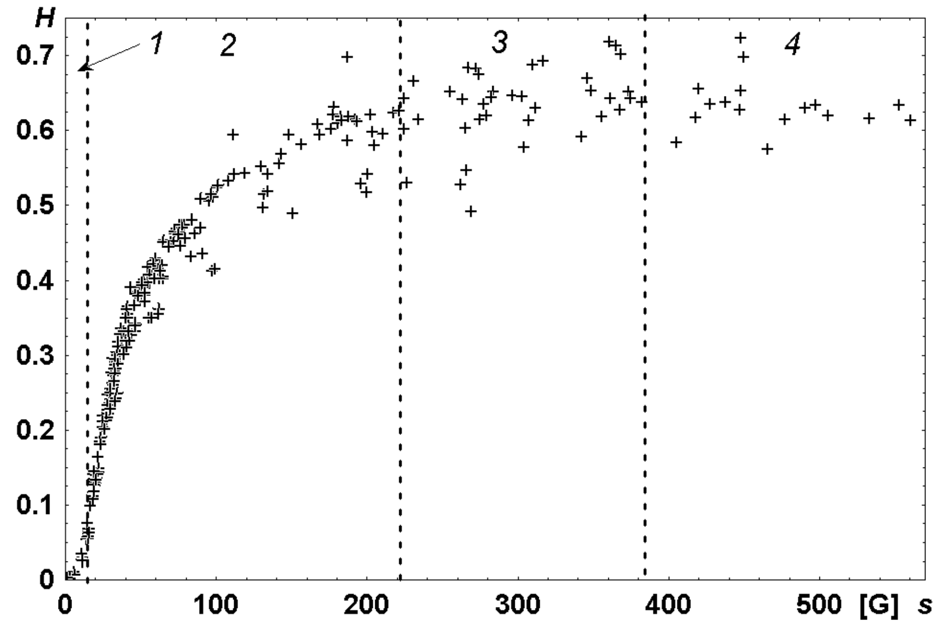

Figure 3. $H(s)$ relation based on the data for the 35-day interval at $d = 10''$: 1) $|B| \leq 50$ G, 2) $2 \leq |B| \leq 2500$ G, 3) $|B| \geq 50$ G, and 4) $|B| \geq 150$ G.

2. Conclusion

Small–scale ($\sim 10''$) stochastic properties of the solar magnetic field B have been analyzed in terms of the model of a fractal Brownian process (described by the Hurst exponent H). The standard deviation s of the magnetic field and the Hurst exponent have been determined at different levels of $|B|$.

The Hurst exponent is much smaller for the background field than for the active region fields.

It is shown that the presence of active regions on the Sun does not, obviously, have a noticeable effect on the small-scale structure of the background magnetic field.

It is established that transition from the background magnetic field to the AR fields takes place at 25–50 G. That is where the magnetic field distribution begins to smooth gradually. The dependence $H(s)$ of the Hurst exponent on the magnetic field amplitude has been derived. After a significant increase, it becomes rather flat at the magnetic field values of the order of hundreds of Gauss (200–300 G).

The results obtained have been related to processes in the solar atmosphere. It is well known that a relatively weak magnetic field inhibits turbulence and turbulent friction in the solar atmosphere, thus, increasing convection and convective heating. This is how a photospheric plage arises (Pikelner 1960). The characteristic fields involved can be estimated from the energy ratio. The equality of the magnetic and kinetic energies (parameter $\beta \approx 1$) corresponds to the field value $B \sim 60$ G. The smoothing of the magnetic field distribution at 25–50 G

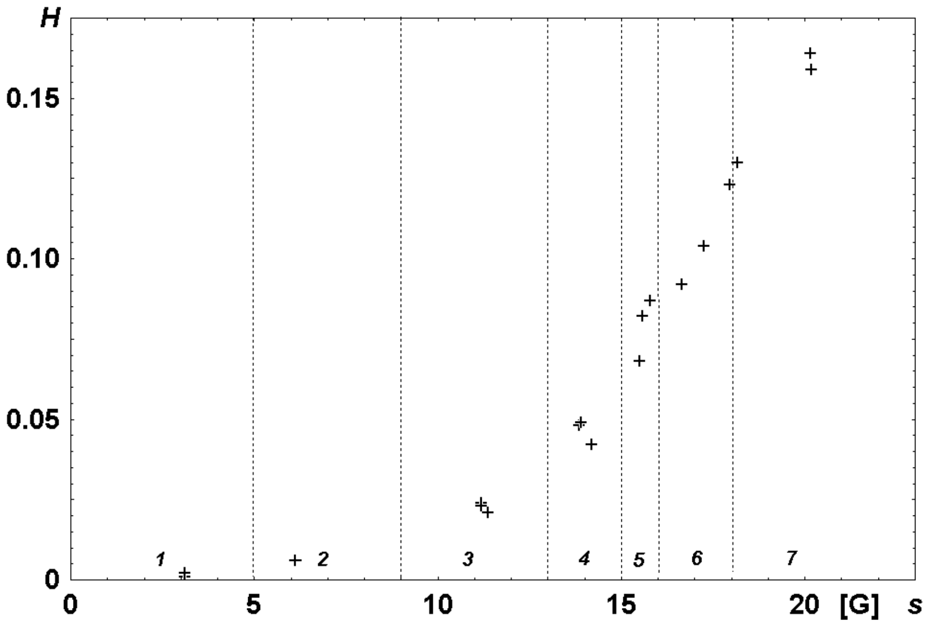

Figure 4. $H(s)$ relation based on the data for three quiet days in 2006 at $d = 10''$: 1) $|B| \leq 3\,\mathrm{G}$, 2) $|B| \leq 10\,\mathrm{G}$, 3) $|B| \leq 25\,\mathrm{G}$, 4) $|B| \leq 50\,\mathrm{G}$, 5) $|B| \leq 100\,\mathrm{G}$, 6) $|B| \leq 200\,\mathrm{G}$, and 7) $|B| \leq 500\,\mathrm{G}$.

can be considered to agree fairly well with the theoretical estimates (Obridko 1985).

Beginning with hundreds of Gauss, the magnetic field inhibits convection (Stepanov & Petrova 1959; Zwaan 1975). The flat part of the plot in Fig. 3 may be considered as representing the region of inhibited convection. Once this limit is reached, the further "smoothing" ceases or slows down significantly.

Acknowledgments. The data from SOHO/MDI were used. SOHO is a project of international cooperation between ESA and NASA.

References

Scherrer, P. H., Bogart, R. S., Bush, R. I., et al. 1995, Solar Phys., 162, 129
Obridko, V. 1985, Sunspots and active solar complexes (Moscow: Nauka)
Pikelner, S. B. 1960, Astronomical J., 37, 616
Potapov, A. A. 2005, Fractals in Radiophysics and Radiolocation, University Book, 463
Stepanov, V. E. & Petrova, N. N. 1959, Izvestija KrAO, 21, 152
Zwaan, C. 1975, Solar Phys., 45, 115